

## Resistance Anomaly and Excess Voltage near Superconducting Interfaces

M. Park, M. S. Isaacson, and J. M. Parpia

*School of Applied and Engineering Physics, and Laboratory of Atomic and Solid State Physics, Cornell University, Ithaca, New York 14853-2501*

(Received 12 June 1995)

We present resistance and current-voltage characteristics of an aluminum film with two regions of different superconducting transition temperatures. The voltage and hence resistance increase above normal state values near the transition. The excess voltage disappears with increasing bias current, accompanied by negative differential resistances. This behavior is associated with the charge imbalance that accompanies normal-superconducting interfaces and phase slip centers.

PACS numbers: 74.80.-g, 74.40.+k, 74.50.+r, 74.60.Jg

The decrease of the resistance from the normal state value is a routine manifestation of the onset of superconductivity. Yet a number of recent publications [1–11] report an anomalous increase in the resistance above the normal state value ( $R_N$ ) in the vicinity of the superconducting transition. This ubiquitous anomaly demands further exploration. Although Kwong *et al.* [1] attributed the resistance anomaly to differences between the nonequilibrium quasiparticle and pair electrochemical potentials ( $\mu_n$  and  $\mu_s$ , respectively), the current-voltage ( $I$ - $V$ ) characteristics and the length scale of the nonequilibrium region were not explored. We report work near  $T_C$  where the nonequilibrium length weakly diverges. Together with the spatial variation of  $T_C$  of our aluminum film, this allows us to place voltage probes within the charge imbalance region. We deduce that the nonequilibrium charge imbalance near normal-superconducting ( $N$ - $S$ ) interfaces and phase slip centers (PSCs) are ultimately responsible for the observed behavior.

We also observe for the first time excess voltage and other features in the  $I$ - $V$  characteristics at dc bias currents above the critical current ( $I_C$ ) [12]. This is likely the result of long quasiparticle relaxation times and interactions between adjacent PSCs [13] whose location and motion is weakly affected by the voltage probes. Throughout the Letter a normal metal ( $N$ ) refers to a superconductor at temperatures above its transition temperature ( $T_C$ ).

Our aluminum film and voltage probes are lithographically patterned in a continuous layer (Fig. 1). The voltage probes,  $1 \mu\text{m}$  wide, are at various distances from the interface between the two regions. The  $T_C$  of the hashed region on the left and of the  $N$  probes is decreased by a few percent through exposure to a  $\text{CF}_4$  reactive ion etch [14]. For this sample,  $T_{C1} = 1.407 \text{ K}$  and  $T_{C2} = 1.452 \text{ K}$  where these refer to the  $T_C$ 's of the etched and unetched film far away from the interface. The thickness and width of the film are  $250 \text{ \AA}$  and  $20 \mu\text{m}$ , respectively. Both regions have nearly identical normal state properties [14]. The resistivity, diffusion constant, elastic mean free path are  $\sim 2 \mu\Omega \text{ cm}$ ,  $\sim 40 \text{ cm}^2/\text{sec}$ , and  $\sim 100 \text{ \AA}$ , respectively.

The residual resistance ratio is  $\sim 2.2$ , and the coherence length  $\xi(T)$  is  $\sim 1 \mu\text{m}$  for the results reported here.

Tunnel junctions are commonly used to decouple the probes from the film. Because of difficulties in integrating tunnel junctions and our etch process, we used narrow voltage probes. Such contacts have been used in the past [2,15,16].  $S$  probes will measure  $\mu_s$  and  $N$  probes measure  $\mu_n$ , although the presence of these probes does locally shift  $T_C$  via the proximity effect. Four terminal measurements are carried out in the earth's magnetic field using a lock-in amplifier to measure  $R$  vs  $T$  at zero dc bias current. The differential resistance ( $dV/dI$  vs  $I$ ) is measured at a fixed temperature with an increasing dc bias current on which a  $0.2 \mu\text{A}$  ac current is superposed.  $I$ - $V$  characteristics are obtained by integrating  $dV/dI$ . (dc techniques yield similar results with lower signal-to-noise ratio.)

Figures 2(a) and 2(b) show  $R$  vs  $T$  data of several sections near the etched-unetched interface. The anomaly is manifested only with  $S$  (unetched) probes (a) and is observed even if the probes do not span the interface, provided they are located within  $\sim \pm 15 \mu\text{m}$  from it.

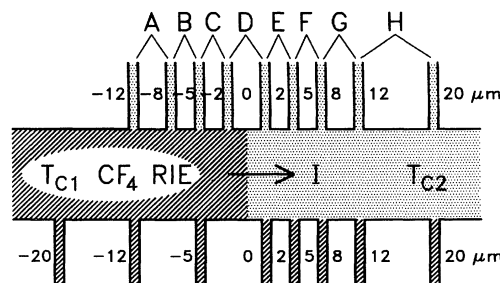


FIG. 1. The aluminum film structure with multiple voltage probes at various distances from the etched-unetched interface. Hashed areas represent regions where the  $T_C$  is decreased. Dotted areas were not exposed to the etch. The interface is designated as the origin; negative positions represent the etched region and the positive positions the unetched region. Each voltage probe is marked with the distance (in  $\mu\text{m}$ ) of its inner edge from the interface. A, B, ..., H refer to sections between the probes.

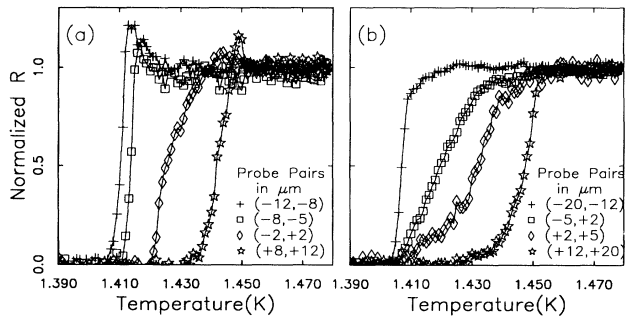


FIG. 2. Resistive transitions at zero bias current. (a) With *S* (unetched) probes the resistance anomaly is observed. Note that the voltage probes need not span the etched-unetched interface in order to observe the anomaly. (b) With *N* (etched) probes, no resistance anomaly is observed.

Figures 3(a) and 3(b) show the unusual  $dV/dI$  and  $I-V$  characteristics at several temperatures just below  $T_{C1}$ . When  $I_C$  is exceeded, a voltage develops rapidly and increases to above  $IR_N$ , consistent with the zero current bias results of Fig. 2(a). As the current is increased further, this excess voltage is given up in increments (see, for example, data at  $T = 1.370$  K), and the voltage eventually approaches the usual normal state Ohmic behavior at high currents. As  $T_C$  is approached, the features are broadened but still present. The incremental decrease in the excess voltage, which manifests itself as a series of negative peaks in  $dV/dI$ , is the nonlocal phenomenon that will be discussed later in this Letter.

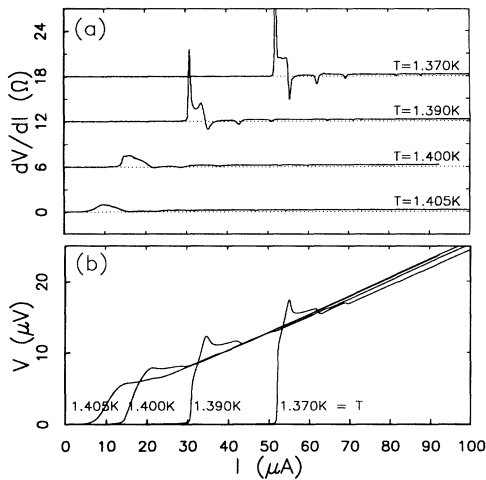


FIG. 3. (a) Behavior of  $dV/dI$  vs  $I$  at several temperatures. Each trace is shifted for comparison. (b)  $I-V$  characteristics obtained by integrating the graphs in (a). The voltage probes are superconducting and located at  $-12$  and  $-8$   $\mu\text{m}$  from the etched-unetched interface. (Both the etched and unetched probes are superconducting since the measurements are performed at temperatures below  $T_{C1}$ ).

When a current flows into a superconductor from a normal region, the quasiparticle distribution is driven away from thermal equilibrium, and this produces a charge imbalance region near the interface. A similar phenomenon occurs around a PSC, which is nucleated at some location where  $I_C$  is locally depressed. The quasiparticles and pairs have different electrochemical potentials within the nonequilibrium region, which extends a distance  $\lambda_{Q^*}$  near the *N-S* interface or around the PSC [17,18]. The difference between the potentials has been directly measured near *N-S* interfaces [15], and around PSCs [12,19]. In aluminum,  $\lambda_{Q^*}$  is long and the resistivity is low. In our film, the estimated  $\lambda_{Q^*}$  is  $\sim 10-20$   $\mu\text{m}$  at  $T = 1.390$  K with an inelastic scattering time of  $\sim 10-40$  ns. The enhancement of  $\lambda_{Q^*}$  due to the proximity to  $T_C$ , together with the gradual spatial inhomogeneity induced around the etched-unetched interface, makes our aluminum film particularly favorable for measurements of nonequilibrium behavior.

If a pair of *S* probes is located around the *N-S* interface [1] and spaced a distance  $a$  apart where  $a < \lambda_{Q^*}$ , then the measured voltage must exceed the normal state value since  $\mu_s$  is constant and set by  $\lambda_{Q^*}$  on the *S* side of the *N-S* interface [20]. In contrast,  $\mu_n$  is a smoothly varying function and does not exceed the normal state value. Thus, a pair of *N* probes would always register a voltage (resistance) less than the normal state value.

Figure 4 shows the spatial variation of  $I_C$ , obtained at two temperatures. The film has a constant  $I_C$  on either side far from the etched-unetched interface. As expected, the etched side has a lower  $I_C$  corresponding to its lower  $T_C$ . The  $T_C$  of the film also shows a similar spatial dependence. Hence, as the temperature is swept from  $T < T_{C1}$  to  $T > T_{C2}$  at zero bias current, the *N-S* interface traverses the film from left to the right of the etched-unetched interface, through sections *A* to *H*. Thus, the resistance anomaly is observed not only with *S* probes located around the etched-unetched interface but also with other pairs of *S* probes [Fig. 2(a)].

We now concentrate on the explanation of the anomaly in the  $I-V$  characteristics, which is successfully modeled

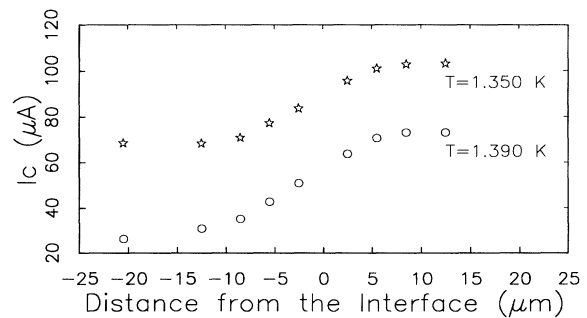


FIG. 4. Spatial variation of  $I_C$  near the etched-unetched interface. Each curve corresponds to a different temperature, and both temperatures are below  $T_{C1}$ .

by the charge imbalance processes around PSCs. As seen in Fig. 4, at low current bias, the entire film is superconducting. With increasing bias current PSCs are sequentially introduced into the film from left to right (consistent with the spatial variation of  $I_C$ ). Because  $I_C$  is locally enhanced near the voltage probes (the film carries current whereas the probes do not), PSCs will preferentially be nucleated between the probes (forming a "cell"). Once a PSC is located in a cell, the  $S$  probes will register a voltage higher than the normal state value  $IR_N$  providing the probe spacing  $a$  is much less than  $\lambda_{Q^*}$ . This follows since the voltage drop around an isolated PSC,  $\Delta\mu_s$ , is  $I_n\rho(2\lambda_{Q^*})$ , where  $I_n$  is the averaged normal current at the center of the PSC and  $\rho$  is the normal resistance per unit length. The higher voltage is a consequence of  $\Delta\mu_s$  being set by  $\lambda_{Q^*}$  and not  $a$ . With higher currents a second PSC enters into the adjacent cell. By symmetry, the nonequilibrium regions between the adjacent PSCs must each be confined to a distance of  $\sim a/2$  from each PSC. Thus, the onset of the second PSC leads to reduction of the voltage and a negative  $dV/dI$  across the first cell.

With this model of anomaly in mind, we focus attention on the  $I$ - $V$  characteristics of section A in Fig. 3. Initially, a PSC is located to the left of probe A reflecting the lower  $I_C$  of that section. When the current exceeds  $I_C$  of section A, PSC<sub>A</sub> is introduced between the pair of probes A, and a voltage that exceeds the normal state develops. With a further increase in current, PSC<sub>B</sub> is introduced in cell B, and the spatial extent of the nonequilibrium region around PSC<sub>A</sub> is curtailed. Thus, the excess voltage is abruptly given up, resulting in a negative  $dV/dI$  peak. (In this model, the voltage ought to revert to the normal state value once PSC<sub>B</sub> is introduced since the nonequilibrium region would be confined to the cell length  $a$ . The disagreement in the data from this expected behavior will be discussed later in the Letter.) With lower temperature, the excess voltage shifts to higher bias currents and the features become sharper. This is in accord with the smaller spatial variations of  $I_C$ , which produce a more rapid introduction of PSCs between the voltage probes and consequent sharper features for a given change in current.

The role of PSCs successfully models the data in Figs. 5(a) and 5(b), which show  $dV/dI$ 's and  $I$ - $V$  characteristics of sections A–H. In trace A, a positive  $dV/dI$  peak and excess voltage is observed as PSC<sub>A</sub> is introduced between the first pair at  $-12$  and  $-8 \mu\text{m}$ . A negative  $dV/dI$  peak is observed when PSC<sub>B</sub> is introduced between the second pair B. At this same bias current, a positive  $dV/dI$  peak and excess voltage is observed in trace B with the introduction of PSC<sub>B</sub>. This sequential behavior is repeated [traces A–F in (a)] until the bias current approaches the spatially constant  $I_C$  value in the region far from the etched-unetched interface. Above this current, all the charge is carried by the quasiparticles. Thus,

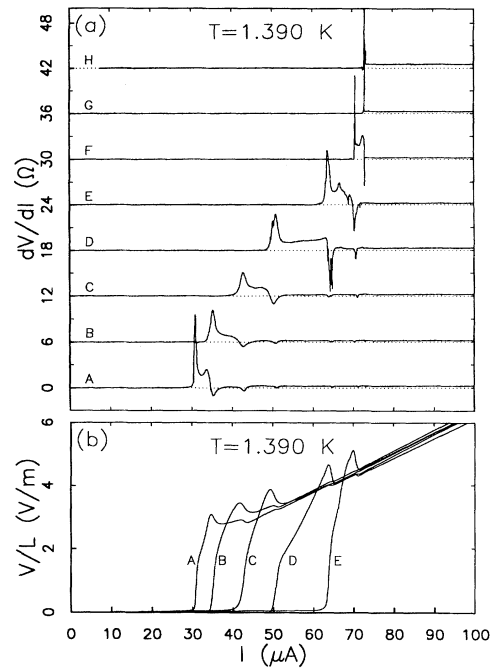


FIG. 5. (a) The  $dV/dI$ 's are measured across sections A–H using pairs of adjacent  $S$  probes at  $T = 1.390 \text{ K}$ . Each trace is shifted for comparison. Trace A corresponds to the voltage across section A, trace B across section B, and so on. (b)  $I$ - $V$  characteristics are obtained from integrating graphs in (a).

neither an excess voltage nor a negative  $dV/dI$  peak is observed [trace G and H in (a)].

We have argued that the excess voltage is a manifestation of the introduction of PSCs. This should produce a single negative  $dV/dI$  peak when the next PSC is nucleated to the right of the sampled region, accompanied by the disappearance of all the excess voltage. However, in Fig. 5(b), the excess voltage persists even after a new PSC is nucleated in the neighboring cell. Also, a series of subsequent smaller  $dV/dI$  features is also observed in Fig. 5(a). [They are also seen in Fig. 3(a).] Comparing traces A–H, it is apparent that these peaks occur when new PSCs are introduced even as far as  $16 \mu\text{m}$  away from the sampled region.

These new nonlocal phenomena can be attributed to the interaction between adjacent PSCs. Since two PSCs within  $\lambda_{Q^*}$  of one another repel, it is likely that when a new PSC is added, it will be located in the right half of its cell since there are no more PSCs to the right. With the addition of this PSC, existing PSCs become more closely packed and are progressively centered within their cells. This leads to a successive and discrete diminution of the excess voltage as the nonequilibrium region around each PSC becomes more confined to its cell. These features associated with the interaction between PSCs are absent in a second experiment on a film with only one pair of  $S$  probes. The excess voltage is smoothly extinguished over

a similar range of bias currents, without the subsequent features in  $dV/dI$ .

We have provided an explanation of the excess voltage and the nonlocal phenomenon in terms of the nucleation and interaction of PSCs. The interactions between PSCs together with the measurement of the excess voltage with probes placed within the charge imbalance region has not been observed previously. The length of the charge imbalance region is accentuated because of the smooth and shallow gradient in  $I_C$  together with long characteristic length scales in our film. In principle, aluminum thin films with modified  $T_C$  should be an ideal system to probe within the nonequilibrium region around phase slip centers. We have also developed an alternative description of the different nonequilibrium potentials  $\mu_s$  and  $\mu_n$  that exist near interfaces and will include this description in a longer paper.

In conclusion, we observe a resistance increase and excess voltage above normal state values near  $T_C$ , together with a nonlocal effect, in an inhomogeneous aluminum film. These observations are explained by the nonequilibrium near  $N$ - $S$  interfaces and around PSCs where differences between  $\mu_n$  and  $\mu_s$  extend over the charge imbalance length. We also observe a new nonlocal phenomenon, which is most likely due to interactions between PSCs. It is reasonable to expect much of the same physics to be present in other inhomogeneous superconducting systems.

We acknowledge helpful conversations with R. Buhrman, V. Ambegaokar, K. Likharev, M. Tinkham, W. Skocpol, V. Petrashov, and B. Janko, together with the suggestion of one of the referees to cast our explanation in terms of the creation of PSCs. The research was supported by the NSF and Cornell MSC Center under Grants No. DRM-9121654 and DRM-9016301. Fabrication was carried out at the Cornell Node of the

Nanofabrication Users Network, supported under Grant No. ECS-8619040.

- 
- [1] Y. K. Kwong *et al.*, Phys. Rev. B **44**, 462 (1991).
  - [2] P. Santhanam *et al.*, Phys. Rev. Lett. **66**, 2254 (1991).
  - [3] J. J. Kim *et al.*, J. Phys. Condens. Matter **6**, 7055 (1994).
  - [4] S. Rubin *et al.*, Ann. Phys. **1**, 492 (1992).
  - [5] R. Vaglio *et al.*, Phys. Rev. B **47**, 15 302 (1993).
  - [6] M. A. Crusellas, J. Fontcuberta, and S. Pinol, Phys. Rev. B **46**, 14 089 (1992).
  - [7] A. Nordstrom and O. Rapp, Phys. Rev. B **45**, 12 577 (1992).
  - [8] E. Spahn and K. Keck, Solid State Commun. **78**, 69 (1991).
  - [9] H. Vloeberghs *et al.*, Phys. Rev. Lett. **69**, 1268 (1992).
  - [10] A. W. Kleinsasser and A. Kastalsky, Phys. Rev. B **47**, 8361 (1993).
  - [11] C. Strunk *et al.*, report, 1995 (to be published).
  - [12] G. J. Dolan and L. D. Jackel, Phys. Rev. Lett. **39**, 1628 (1977).
  - [13] M. Tinkham, J. Low Temp. Phys. **35**, 147 (1979).
  - [14] M. Park *et al.*, J. Vac. Sci. Technol. A **13**, 127 (1995).
  - [15] M. L. Yu and J. E. Mercereau, Phys. Rev. B **12**, 4909 (1975).
  - [16] J. Clarke, Phys. Rev. Lett. **28**, 1363 (1972).
  - [17] J. Clarke, in *Nonequilibrium Superconductivity, Phonons, and Kapitza Boundaries*, edited by K. E. Gray (Plenum, New York, 1981), and references therein.
  - [18] W. J. Skocpol, M. R. Beasley, and M. Tinkham, J. Low Temp. Phys. **16**, 145 (1974).
  - [19] M. Stuiyinga *et al.*, J. Low Temp. Phys. **53**, 633 (1983).
  - [20] A complete treatment should account for the presence of the equilibrium proximity effect as well as the nonequilibrium charge imbalance. Since  $\lambda_Q^* > \xi(T)$ , we have neglected the proximity effect in this discussion.